Two distinct mechanisms of coherence in randomly perturbed dynamical systems

R. E. Lee DeVille and Eric Vanden-Eijnden
Courant Institute of Mathematical Sciences, New York University, New York, New York 10012, USA

Cyrill B. Muratov
Department of Mathematical Sciences, New Jersey Institute of Technology, Newark, New Jersey 07102, USA
(Received 10 May 2005; published 14 September 2005)

We carefully examine two mechanisms—coherence resonance and self-induced stochastic resonance—by which small random perturbations of excitable systems with large time scale separation may lead to the emergence of new coherent behaviors in the form of limit cycles. We analyze what controls the degree of coherence in these two mechanisms and classify their very different properties. In particular we show that coherence resonance arises only at the onset of bifurcation and is rather insensitive against variations in the noise amplitude and the time scale separation ratio. In contrast, self-induced stochastic resonance may arise away from bifurcations and the properties of the limit cycle it induces are controlled by both the noise amplitude and the time scale separation ratio.

DOI: 10.1103/PhysRevE.72.031105 PACS number(s): 05.40.−a, 02.50.Fz, 42.60.Rn

I. INTRODUCTION

Understanding the effect of random perturbations on nonlinear dynamical systems is a challenge across many disciplines of science. These perturbations may be small and irrelevant, or may be so large as to overwhelm the dynamics. More interestingly, they can be small and yet result in profound qualitative changes in the system behavior without introducing any significant randomness [1,2]. This observation has attracted a lot of attention recently because of its relevance, e.g., in biological systems (see, e.g. [3–6]).

An important class of nonlinear dynamical systems in which this phenomenon may occur are excitable systems. Excitable systems arise in a wide variety of areas which include climate dynamics, semiconductors, chemical reactions, lasers, combustion, neural systems, cardiovascular tissues, etc. and are especially common in biology [7–9]. A canonical example of a biological excitable system is a nerve cell. The defining property of all these systems is the way they respond to perturbations. If a perturbation is sufficiently small, the system quickly relaxes back into the unique stable steady state. On the other hand, once the perturbation reaches a certain threshold, a large transient response (as, e.g., an action potential in nerve cells) is triggered before the system recovers to its steady state.

Noise-driven excitable systems can produce dynamical responses which possess a high degree of coherence and yet are significantly different from what is observed in the absence of noise. One mechanism by which this phenomenon can occur is coherence resonance (CR). It was first proposed in the work of Pikovsky and Kurths [10] and since then attracted considerable attention (see, e.g. [11–19], and also [20] for a recent extensive review). In CR, a dynamical system near but before Hopf bifurcation threshold is driven by small noise towards the deterministic limit cycle which emerges right after the bifurcation. Very recently, an alternative mechanism, termed self-induced stochastic resonance (SISR), has been proposed [21]. In SISR small random perturbations also lead to the emergence of a coherent limit cycle behavior, but in a profoundly different way and with different properties than in CR (see also [22]).

The purpose of this paper is to give a detailed analysis of CR and SISR, carefully establish when and why these mechanisms occur, and distinguish the different properties of the limit cycles they induce. In particular, we characterize what controls the degree of coherence of these noise-induced limit cycles, and under what conditions their coherence can be made arbitrarily large, leading to an essentially *deterministic* behavior out of noise.

To this end, we will focus on the FitzHugh-Nagumo model. This model is often considered as a minimal caricature of more realistic models of excitable systems (see, e.g., [7]). We study the following version of the FitzHugh-Nagumo model perturbed by noise:

$$\varepsilon \dot{x} = x - \tfrac{1}{3}x^3 - y + \sqrt{\varepsilon}\,\delta_1 \dot{W}_1, \tag{1a}$$

$$\dot{y} = x + a + \delta_2 \dot{W}_2, \tag{1b}$$

where a, ε, δ_1, and δ_2 are positive constants, and $\dot{W}_1$ and $\dot{W}_2$ are independent standard white-noises. With δ_1 set to zero, Eqs. (1a) and (1b) become precisely the original system studied by Pikovsky and Kurths in their pioneering paper on CR [10]. With $\delta_2 = 0$ instead, (1a) and (1b) display SISR [21], as we will show below.

At first sight, one may suppose that the noise will have a similar effect regardless of whether it is added to (1a) or (1b), or both. And yet numerical solutions of (1a) and (1b) shown in Figs. 1 and 2 reveal a marked difference between the two, especially at smaller values of ε [36].

Figure 1 shows the histograms of the time interval T between the successive oscillations in x obtained from the numerical solution of the stochastic differential equations (1a) and (1b) for $a = 1.05$, with $\varepsilon = 10^{-2}$ in the upper two panels, Figs. 1(a) and 1(b), and with $\varepsilon = 10^{-4}$ in the lower two panels, Figs. 1(c) and 1(d). In the left two panels, Figs. 1(a) and 1(c), we take $\delta_1 = 0, \delta_2 = 0.2$, leading to CR. In the right two pan-

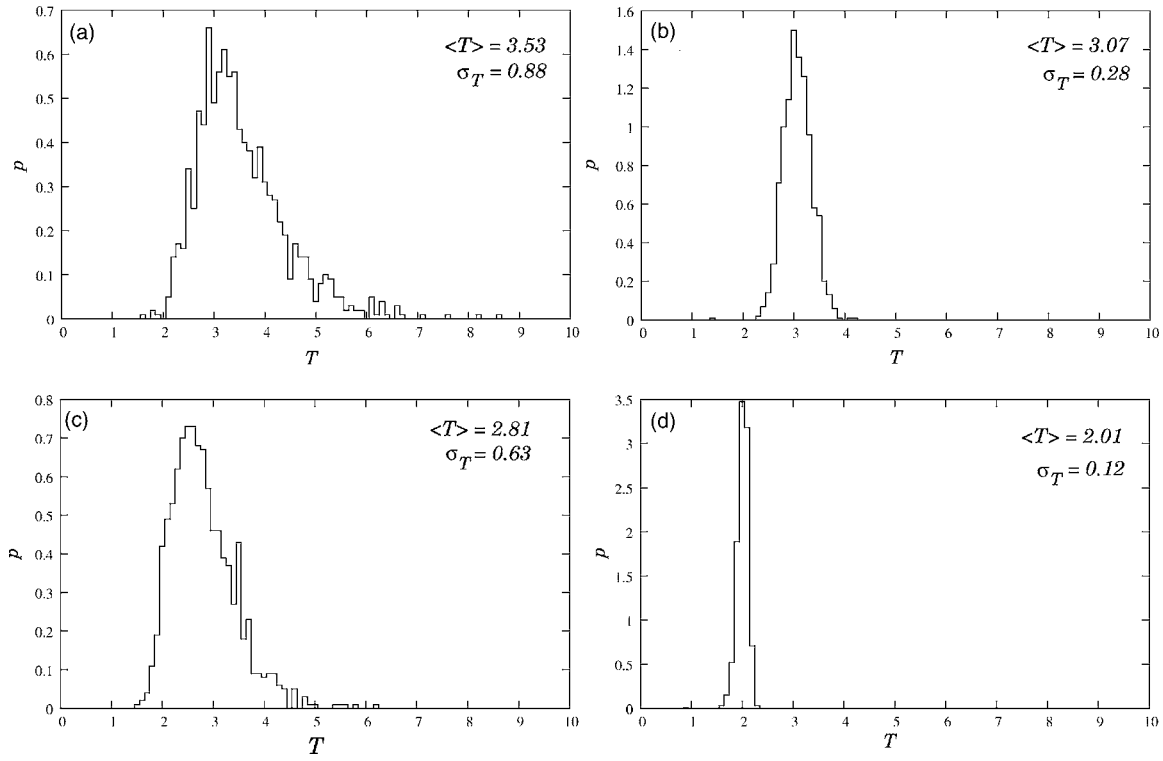

FIG. 1. The histograms of the time interval T between successive oscillations in x obtained from numerical solution of (1) with $a=1.05$. (a) $\varepsilon=10^{-2}, \delta_1=0, \delta_2=0.2$ (CR); (b) $\varepsilon=10^{-2}, \delta_1=0.2, \delta_2=0$ (SISR); (c) $\varepsilon=10^{-4}, \delta_1=0, \delta_2=0.2$ (CR); (d) $\varepsilon=10^{-4}, \delta_1=0.2, \delta_2=0$ (SISR).

els, Figs. 1(b) and 1(d), we take $\delta_1=0.2, \delta_2=0$, leading to SISR. In agreement with the general CR mechanism (see Sec. III), one can see from Figs. 1(a) and 1(c) that the statistics of T are rather insensitive to the time scale separation ratio when the noise is added only to (1b) and not to (1a). In contrast, SISR (see Sec. IV) is sensitive to the time scale separation ratio and one sees a significant difference between Figs. 1(b) and 1(d); in the latter the degree of coherence has dramatically increased and, furthermore, the average period $\langle T\rangle$ of oscillations decreased by a factor of 1.5, far exceeding the uncertainty in T, as measured by its standard deviation σ_T.

This difference is also observed in the time series and phase portrait of the numerical solutions which are shown in Figs. 2. The difference between Fig. 2(a), showing an instance of CR, and Fig. 2(b), showing an instance of SISR, is striking. In the case of CR, the limit cycle is essentially a precursor of a deterministic limit cycle obtained upon crossing the Hopf bifurcation in the limit $\varepsilon\to 0$. In contrast, the limit cycle in SISR does not follow any trajectory that exists in the system's deterministic dynamics for any parameters, yet it shows remarkable coherence in period (substantially greater than in the case of CR for the same parameters) despite a noticeable effect of noise on the trajectories.

The remainder of this paper is devoted to explaining the differences in the observations above and clarifying the nature of both mechanisms by presenting an asymptotic theory of these noise-induced phenomena in the limit of perfect coherence. Since the condition $\varepsilon \ll 1$ of strong time scale separation is required for both CR and SISR [10,21], we will assume it in all the arguments below.

The paper is organized as follows. In Sec. II we summarize the properties of the noise-free system in (1a) and (1b) with strong time scale separation. In Sec. III we consider the situation in which the CR mechanism becomes perfectly coherent. In Sec. IV we present an asymptotic theory of SISR in the considered model. In Sec. V we consider the behavior of SISR near the threshold of the Hopf bifurcation. In Sec. VI we analyze what happens if noise terms are added to both equations in (1a) and (1b). Finally we draw some conclusions in Sec. VII.

II. THE DETERMINISTIC DYNAMICS

In this section we briefly recall the main features of the deterministic system in (1a) and (1b):

$$\varepsilon\dot{x} = x - \tfrac{1}{3}x^3 - y, \tag{2a}$$

$$\dot{y} = x + a, \tag{2b}$$

for $\varepsilon \ll 1$ (see, e.g., [23,24]). Since (2a) and (2b) are invariant under the transformation $(x,y,a)\to(-x,-y,-a)$, we do not need to consider the case $a<0$ separately. The system in (2a) and (2b) has a unique fixed point at $(x,y)=(x_\star,y_\star)$, where

$$x_\star = -a, \quad y_\star = -a + \tfrac{1}{3}a^3. \tag{3}$$

Linearizing (2a) and (2b) around the fixed point with respect to the functions $x=x_\star+c_1e^{-\gamma t}, y=y_\star+c_2e^{-\gamma t}$, we find that $\gamma=\gamma_\pm(a)$, with

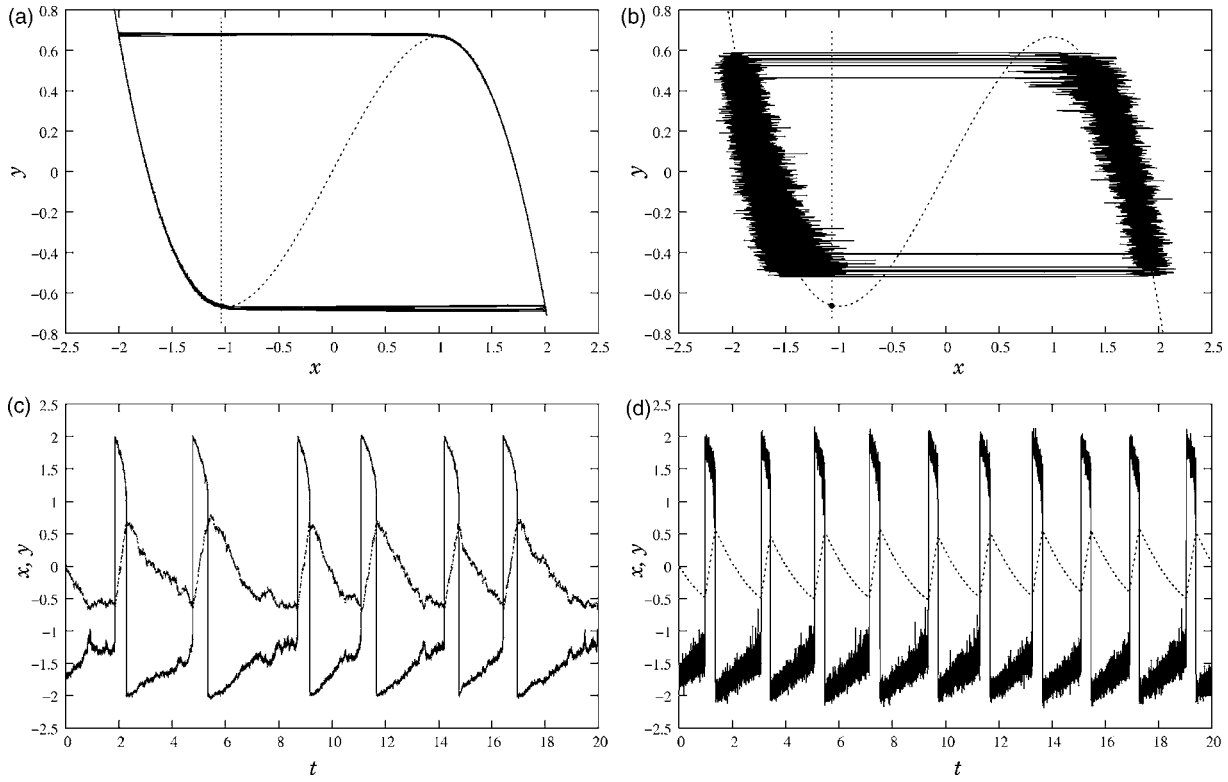

FIG. 2. Two types of limit cycle behaviors observed in the numerical simulations of (1a) and (1b) with $a=1.05$. (a) and (c): $\varepsilon=10^{-4}, \delta_1=0, \delta_2=0.2$ (CR); (b) and (d): $\varepsilon=10^{-4}, \delta_1=0.2, \delta_2=0$ (SISR). In (a) and (b), the phase portrait is shown, whereas in (c) and (d), the time traces of both x and y are shown. In 2(a) and 2(b), the dotted lines indicate the nullclines.

$$\gamma_{\pm}(a)=\frac{a^2-1\pm\sqrt{(a^2-1)^2-4\varepsilon}}{2\varepsilon}. \tag{4}$$

Therefore, the fixed point is stable if and only if $|a|>1$ and, in fact, is globally attracting. At $a=1$ the system undergoes a Hopf bifurcation, and so for all $|a|<1$ there exists a limit cycle which is globally stable [25]. Note that a peculiar feature of systems with strong time scale separation is that the normal form expansion near a bifurcation point is valid only in a very small neighborhood of the bifurcation [17,18]. For this reason the fixed point becomes a stable node rather than a focus for $a>a_N$, where

$$a_N=\sqrt{1+2\varepsilon^{1/2}}=1+O(\varepsilon^{1/2}), \tag{5}$$

see Eq. (4). Also, for the same reason the limit cycle has *large* amplitude when a approaches 1 from above provided that $\varepsilon\to 0$ sufficiently fast [26,27].

When $|a|<1$ and $\varepsilon\to 0$, the motion on the limit cycle is broken up into fast and slow motions [23,24]. We define S_L to be the attracting branch of the x nullcline where $y=x-\frac{1}{3}x^3$ on the left, defined for $x\in(-\infty,-1)$, and S_R to be the attracting branch on the right, defined for $x\in(1,\infty)$. During slow motions [on the $O(1)$ time scale] the trajectory follows S_L and S_R:

$$\text{Slow:}\quad \dot{x}=\frac{x+a}{1-x^2},\quad y=x-\tfrac{1}{3}x^3. \tag{6}$$

This is followed by abrupt jumps [on the $O(\varepsilon)$ time scale] from S_L to S_R and back, when the trajectory reaches the respective knees of S_L and S_R, located at $(-1,-\frac{2}{3})$ and $(1,\frac{2}{3})$:

$$\text{Fast:}\quad \varepsilon\dot{x}=x-\tfrac{1}{3}x^3-y,\quad y=\pm\tfrac{2}{3}. \tag{7}$$

See Fig. 3 for a summary. Since the trajectory spends most of the time in the slow motions, the period of the limit cycle is asymptotically the time spent on S_L and S_R in one cycle:

$$T_{LC}(a)=\int_{-2}^{-1}\frac{1-x^2}{x+a}dx+\int_{2}^{1}\frac{1-x^2}{x+a}dx \tag{8}$$

$$=3-(1-a^2)\ln\left(\frac{4-a^2}{1-a^2}\right). \tag{9}$$

As was already noted above, when a approaches the point of the Hopf bifurcation of $(x_\star,y_\star)$, in the limit $\varepsilon\to 0$ (taken first) we have

$$\lim_{a\to 1-}T_{LC}(a)=3, \tag{10}$$

which is different from $2\pi/\omega_0$, where $\omega_0=\mathrm{Im}\,\gamma_+(1)=\varepsilon^{-1/2}$ is the frequency at the onset of the Hopf bifurcation (for more detailed discussion, see [17,18]).

In contrast, when $|a|>1$, the system in (2a) and (2b) is excitable (for a general discussion of excitability and its ap-

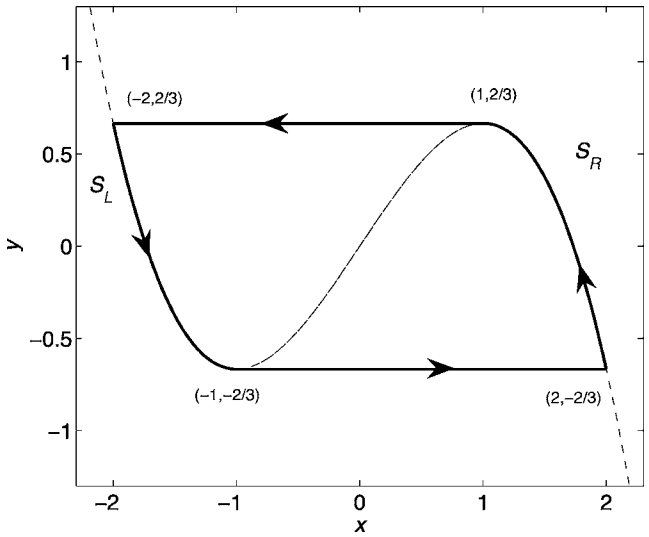

FIG. 3. Phase plane portrait for (2) with $|a|<1$ in the limit $\varepsilon \to 0$. The limit cycle is shown by the thick solid lines with arrows. Dashed line indicates the x nullcline.

plications see, e.g. [7,28,29]). This can be seen from the phase portrait shown in Fig. 4. In this case, starting with an arbitrary initial condition, the trajectory is quickly attracted to either S_L or S_R. If the initial condition is such that the trajectory reaches S_L first by the fast motion, it subsequently slides along S_L towards the fixed point $(x_\star, y_\star)$, where it settles forever. If, however, the initial condition is such that the trajectory reaches S_R first, it then slides upward along S_R towards the knee at $(x,y)=(1,\frac{2}{3})$, which it reaches in finite time, then jumps to S_L, and proceeds as before. Therefore, small perturbations around the fixed point will decay right back to the fixed point, while sufficiently large deviations from the fixed point will result in transient large-amplitude excursions before the system returns to the fixed point. Next we analyze how this picture changes with the inclusion of a small random perturbation.

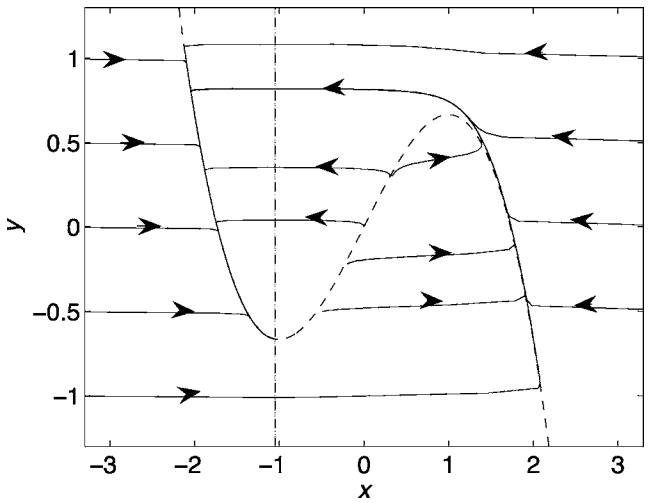

FIG. 4. Phase plane portrait of the deterministic system (2a) and (2b) with $a=1.05$ and $\varepsilon=0.01$. The dashed lines show the nullclines.

III. COHERENCE RESONANCE

Following [10], consider (1a) and (1b) with $\delta_1=0$ and $a>1$:

$$\varepsilon \dot{x} = x - \tfrac{1}{3}x^3 - y, \tag{11a}$$

$$\dot{y} = x + a + \delta_2 \dot{W}_2. \tag{11b}$$

As was shown in [10], for certain choices of parameters this systems of stochastic differential equations exhibits coherent limit cycle behavior (see also early work [30]). In fact, in a suitable limit of the control parameters ε, a, and δ_2, the solutions of (11a) and (11b) follow *precisely* the deterministic limit cycle discussed in Sec. II when $a \to 1-$, as we now show.

Let us see what conditions the emergence of this cycle requires. First, one needs that the noise amplitude is small enough, $\delta_2 \to 0$. The limiting behavior cannot be deterministic otherwise. As soon as $\delta_2 \to 0$, one realizes that one must also have $a \to 1+$, i.e., in the limit the deterministic system in (2a) and (2b) must be at bifurcation threshold. Indeed, if the noise in (11b) is vanishingly small, $\delta_2 \to 0$, but $a=1+O(1)$ and $\varepsilon \ll 1$ fixed, then large excursions (defined, e.g., as those which reach $x=0$) of the trajectory away from the fixed point only occur on exponentially long time scale $O(e^{c\delta_2^{-2}})$ and are random with Poisson statistics (this results from large deviation theory [1]). If $\delta_2 \to 0$, no coherent oscillations are therefore possible if $|a|$ is bounded away from 1.

On the other hand, the noise can destabilize the point $(x_\star, y_\star)$ if this point is near the onset of instability to begin with, i.e. $(x_\star, y_\star) \to (-1, -\frac{2}{3})$, and this requires that $a \to 1+$ and $\delta_2 \to 0$ jointly. Now, in order for the noise to act as soon as the trajectory reaches $(x_\star, y_\star)$, that is, in order to avoid that the trajectory stick to this point for too long and lose coherence, one has to require that the noise be bounded below by a function of $a-1$. More specifically, we show that one needs

$$\delta_2 \geqslant C_1 \left(\frac{b^3}{\ln b^{-1}} \right)^{1/2}, \quad b = a - 1, \tag{12}$$

for some constant $C_1 > 0$ when $\delta_2 \to 0$ and $b \to 0+$. To see this, we look at the picture locally around the fixed point by rescaling the variables as

$$\xi = b^{-1}(x+a), \quad \eta = b^{-2}(y + a - a^3/3), \quad t = bs. \tag{13}$$

Using (13) and letting $0 < b \ll 1$, we rewrite (11) to leading order as

$$d\xi = b^2 \varepsilon^{-1}(-2\xi - \eta + \xi^2) ds, \tag{14a}$$

$$d\eta = \xi ds + \delta_2 b^{-3/2} dW_s. \tag{14b}$$

One can check that the knee of S_L is now asymptotically at $(\xi, \eta)=(1,-1)$, and the ξ nullcline is a quadratic function with minimum at $(1,-1)$ and zeros at $\xi=0,2$; see Fig. 5. By direct inspection of (14a) and (14b), we immediately conclude that $\delta_2 b^{-3/2}$ must not go to zero in this scaling. Indeed, assume for simplicity that $a > a_N$, or, equivalently, that $b \gtrsim O(\varepsilon^{1/2})$. Then the deterministic dynamics governed by (14a) and (14b) has a separatrix between the trajectories that

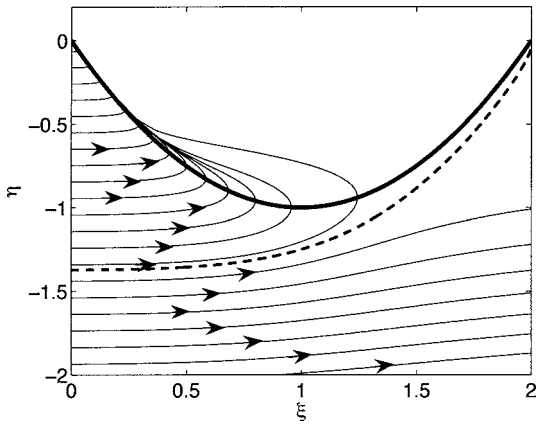

FIG. 5. Blowup of the deterministic trajectories near the fixed point when $\varepsilon b^{-2}=0.1$. The x nullcline is shown by the thick solid line. The separatrix is shown by the thick dashed line.

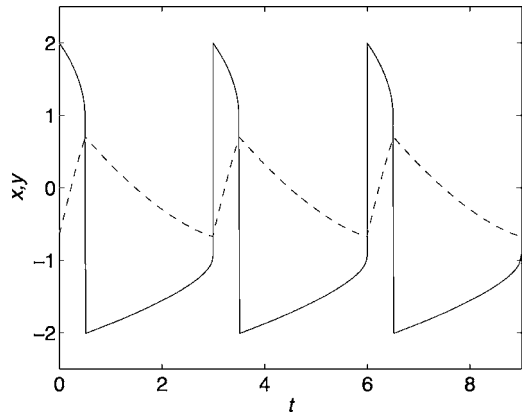

FIG. 6. Asymptotic limit cycle in CR. The solid lines show $x(t)$ and the dashed lines show $y(t)$ obtained from matching the fast and slow motions.

terminate at the fixed point and the trajectories that run off to infinity in finite time; see Fig. 5 [37]. Since the origin is an attracting fixed point and the system needs to travel at least to the separatrix to escape this fixed point, if the noise level is too small [i.e., when (12) is not satisfied], then the time τ to reach the separatrix will grow exponentially as

$$\tau \sim be^{cb^3\delta_2^{-2}} \to \infty, \tag{15}$$

despite $b \to 0$. Of course, coherence of the trajectories will be lost in this case. So, the condition in (12) is necessary in order to avoid this.

In contrast, if $\delta_2 \gtrsim b^{3/2}$, it does not matter when and where the trajectory escapes the vicinity of the fixed point. Indeed, this will happen with probability 1 at finite s. But $t=bs$, and so anything which happens in a finite s time takes place in zero time in the t time scale.

Once away from the fixed point and the left knee, the trajectory will not be affected appreciably by the noise since $\delta_2 \to 0$. Just as in the case of the deterministic limit cycle considered in Sec. II, the trajectory will follow a fast motion described by (7) and land near the point $\left(2,-\frac{2}{3}\right)$ on S_R in $O(\varepsilon)$ time. It then moves up S_R to reach the right knee at $\left(1,\frac{2}{3}\right)$ in asymptotic time

$$T_{LC}^R = \int_2^1 (1-x)dx = \tfrac{1}{2}, \tag{16}$$

which is obtained by integrating (6) with $a=1$. After that, the trajectory falls off onto S_L at $\left(-2,\frac{2}{3}\right)$ and travels along S_L until it approaches the fixed point. Thus, what makes the CR mechanism work is the fact that in the limit $\varepsilon \to 0, a \to 1+$, and $\delta_2 \to 0$ (in this order) the time to reach an arbitrary fixed neighborhood of $(x_\star, y_\star)$ is finite (see also [31]):

$$T_{LC}^L = \int_{-2}^{-1} (1-x)dx = \tfrac{5}{2}. \tag{17}$$

Once the trajectory enters a small neighborhood of the fixed point, it will then take $O(b) \ll 1$ time to escape it to complete the cycle, in the limit resulting in a deterministic limit cycle with period

$$T_{CR} = T_{CR}^R + T_{CR}^L = 3, \tag{18}$$

which is essentially the same as the one constructed in Sec. II in the absence of the noise in the limit $a \to 1-$; see Figs. 3 and 6. Thus, the coherent limit cycle behavior one gets for $a>1$ and $\delta_2 \ll 1$ is a precursor to the deterministic limit cycle appearing for $a<1$.

Summarizing, CR arises provided that

$$\varepsilon \ll 1, \quad \varepsilon^{1/2} \lesssim b \ll 1, \quad b^{3/2} \lesssim \delta_2 \ll 1. \tag{19}$$

The predicted limit cycle agrees well with the numerics shown in Fig. 2; compare, e.g., Figs. 3 and 6 with Figs. 2(a) and 2(c).

Finally we note that the scaling $b \gtrsim \varepsilon^{1/2}$ which we chose for convenience is sufficient to create coherence resonance, but it may not be necessary. In particular, coherence may also occur in the narrow range $0<b \ll \varepsilon^{1/2}$ [17,18], but the stochastic system is quite complicated to analyze in this limit.

IV. SELF-INDUCED STOCHASTIC RESONANCE

Consider now (1a) and (1b) with $\delta_2=0$:

$$\varepsilon \dot{x} = x - \tfrac{1}{3}x^3 - y + \sqrt{\varepsilon}\delta_1 \dot{W}_1, \tag{20a}$$

$$\dot{y} = x + a. \tag{20b}$$

The scaling $\sqrt{\varepsilon}\delta_1$ guarantees that δ_1 measures the relative strength of the noise term compared to the deterministic term $x-\frac{1}{3}x^3-y$ irrespective of the value of ε.

As was shown in [21], noise-driven excitable systems described by equations of the type of (20a) and (20b) can also lead to a deterministic limit cycle in the limit as $\delta_1 \to 0$ and $\varepsilon \to 0$. However, the SISR mechanism by which this is achieved is somewhat more subtle than that of CR, and the properties of the limit cycle in SISR are very different from the ones in CR. Let us point out that the idea of SISR was

first introduced by Freidlin for a model of a noise-driven mechanical system in Ref. [22] (see also related early work in Refs. [32,33] in the context of stochastic resonance [34]).

In SISR, it is *not* required that $a \to 1+$. In fact, one can choose any $1 < a < \sqrt{3}$ and thus be far away from the bifurcation threshold. Furthermore, the limit cycle is *not* the deterministic one obtained in the limit as $a \to 1-$, and both its phase portrait and its period can be controlled by a parameter depending on δ_1 and ε. Next we explain why this is so with an asymptotic argument.

As in CR, we require that $\delta_1 \to 0$ since this is the only way to obtain a deterministic solution. We also let $\varepsilon \to 0$. Then there exists an open interval $I(a)$, which depends on a, so that if

$$\delta_1^2 \ln \varepsilon^{-1} \to C_2 \tag{21}$$

for some constant $C_2 \in I(a)$ as $\delta_1 \to 0$ and $\varepsilon \to 0$, a deterministic limit cycle emerges. This limit cycle can be understood as the result of keeping the system in a state of perpetual frustration. The system tries to reach the fixed point $(x_\star, y_\star)$ by sliding down S_L, but each time it gets kicked by the noise towards S_R before reaching $(x_\star, y_\star)$. The system then slides up S_R, gets kicked toward S_L before reaching the knee, and again starts sliding down toward $(x_\star, y_\star)$. It can then repeat this cycle.

To understand the jumping mechanism, we first make the change of variables $t = \varepsilon \tau$, to get

$$dx = \left(x - \tfrac{1}{3}x^3 - y\right)d\tau + \delta_1 dW_\tau, \tag{22a}$$

$$dy = \varepsilon(x + a)d\tau. \tag{22b}$$

Equation (22a) is of the form

$$dx = -\frac{\partial V(x,y)}{\partial x}d\tau + \delta_1 dW_\tau,$$

where V is a double-well potential

$$V(x,y) = -\tfrac{1}{2}x^2 + \tfrac{1}{12}x^4 + xy. \tag{23}$$

Since y is nearly constant on this time scale from (22b), y enters merely as a parameter in (23). Viewed as a function of x with y fixed, $V(x,y)$ is a double-well potential with two minima located at the value of x where S_L and S_R intersect the horizontal line $y = \text{const}$, and a maximum at the intersection with the unstable branch of the x nullcline (see Fig. 7). To be more precise, let us define, for $y \in \left(-\frac{2}{3}, \frac{2}{3}\right)$, the three roots

$$x_-(y) < x_0(y) < x_+(y)$$

of $y = x - \frac{1}{3}x^3$. The points $x_\pm(y)$ are always local minima of the potential, and $x_0(y)$ is a local maximum. We define

$$\Delta V_+(y) = V(x_0(y), y) - V(x_+(y), y),$$

$$\Delta V_-(y) = V(x_0(y), y) - V(x_-(y), y).$$

In each case, $\Delta V_\pm(y)$ is the potential difference between the local maximum $x_0(y)$, and a local minimum $x_\pm(y)$, see Fig. 7. The value of $\Delta V_+(y)$ can be easily computed parametrically

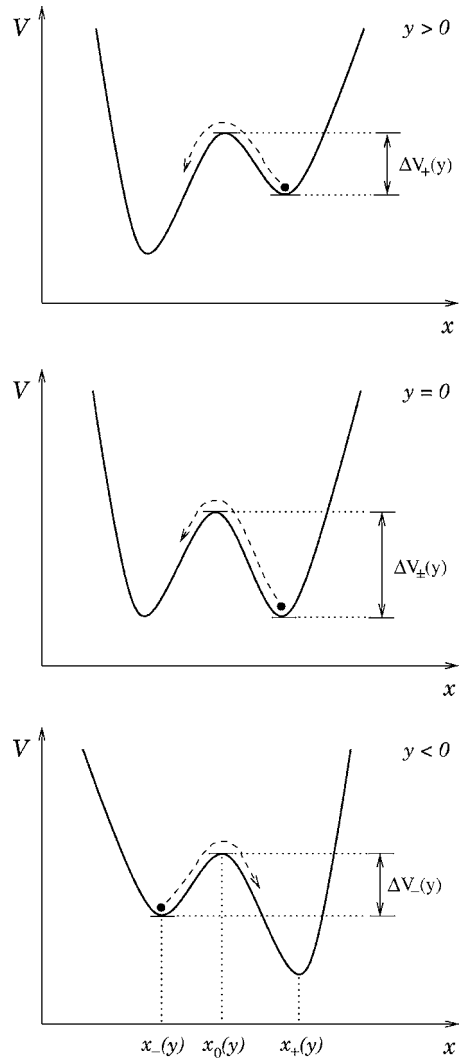

FIG. 7. Schematics of the potential $V(x,y)$ for different values of y.

in terms of $x_1 = x_+(y)$. After some straightforward algebra, we have

$$\Delta V_+ = -\frac{3}{4} + \frac{\sqrt{3}}{8}x_1(4 - x_1^2)^{3/2} - \frac{3}{8}x_1^2(2 - x_1^2), \tag{24}$$

and by symmetry $\Delta V_-(y) = \Delta V_+(-y)$. The resulting curves are plotted in Fig. 8.

Going back to (22a) and (22b), fix $y > 0$ and choose x near S_R. This puts x in the basin of attraction of $x_+(y)$ (right well). Due to the noise, the process can jump into the left well by hopping over the barrier. Since the potential barrier it needs to cross is of size $\Delta V_+(y)$, from Wentzell-Freidlin theory [1] we know that the crossing time will asymptotically be a Poisson process with intensity

$$\lambda(y) = C \exp(-2\Delta V_+(y)/\delta_1^2), \tag{25}$$

where C is some prefactor. By this we mean that for large T, the probability of seeing a jump over the barrier is

$$\text{Prob(jump at } y) = 1 - e^{-\lambda(y)T}.$$

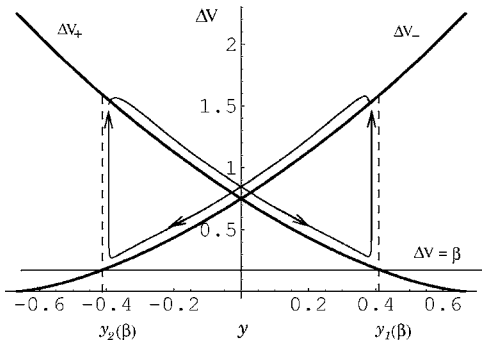

FIG. 8. Barrier heights $\Delta V_{\pm}$ as function of y. The motion along S_L and S_R followed by jumps between the two is indicated by the arrows. The curves $\Delta V_{\pm}(y)$ intersect at $\Delta V=\beta_{c2}=\frac{3}{4}$.

Now let y vary using (22b). One can see that the time scale for y to move along S_R deterministically is ε^{-1}. If the two time scales happen to match at some point $y=y_1$, then we will expect a jump at this point y_1. Indeed, before the trajectory reaches y_1, the motion on S_R is infinitely faster than the time scale of the jump, and hence this jump is not observed. But as soon as the trajectory passes y_1, the situation is reversed: the time scale of the jump becomes infinitely faster than the motion on S_R and hence the jump happens instantaneously at y_1. From (25), the matching of time scales requires that

$$\varepsilon^{-1} \approx \lambda(y_1) = C \exp(2\Delta V_+(y_1)/\delta_1^2),$$

and so we must let $\delta_1 \to 0, \varepsilon \to 0$ so that

$$\frac{1}{2}\delta_1^2 \ln(\varepsilon^{-1}) \to \Delta V_+(y_1).$$

Notice that to leading order the prefactor C in the intensity (25) is irrelevant to determine y_1

Let us justify this formal argument (see also [22]). Consider a sequence such that

$$\frac{1}{2}\delta_1^2 \ln\, \varepsilon^{-1} \to \beta,$$

and say that y_1 is such that $\Delta V_+(y_1)=\beta$. Then we claim that with probability asymptotically close to 1, the system follows S_R until it reaches $y=y_1$, after which it jumps to S_L. We argue as follows: take $(x_+(y), y)$ for some $y<y_1$, and let this point evolve according to (22a) and (22b). Fix $dy>0$ small [but $O(1)$ in ε], then one of two things can happen: either the noise kicks the trajectory to S_L before it reaches $y+dy$, or the system evolves deterministically to $y+dy$ and stays near S_R. The time we would wait to evolve from y to $y+dy$ is $C\varepsilon^{-1}dy$, whereas the intensity is

$$\lambda(y) = C \exp(-2\Delta V_+(y)\delta_1^{-2}) \to C\varepsilon^{\Delta V_+(y)/\beta}.$$

Thus the probability of jumping before reaching $y+dy$ is

$$\text{Prob(jump between } y \text{ and } y+dy) = 1 - \exp(-\lambda(y)C\varepsilon^{-1}dy)$$
$$= 1 - C\exp(-\varepsilon^{(\Delta V_+(y)-\beta)/\beta}).$$

For $\Delta V_+(y)>\beta$, the second term above is exponentially close to 1, so the probability to jump is exponentially close to 0. Similarly, the probability of jumping is exponentially close to 1 for $\Delta V_+(y)<\beta$. Since $\Delta V_+(y)$ is a monotone decreasing function of y (see Fig. 8), the system will, with probability exponentially close to 1, traverse S_R until it reaches $y=y_1$, at which time it jumps to S_L. The same argument will hold for a trajectory on S_L, with the modification that the potential barrier is then $\Delta V_-(y)$, so the trajectory jumps to the right at the point $y=y_2$, where $\Delta V_-(y_2)=\beta$. Of course, by symmetry $y_2(\beta)=-y_1(\beta)$.

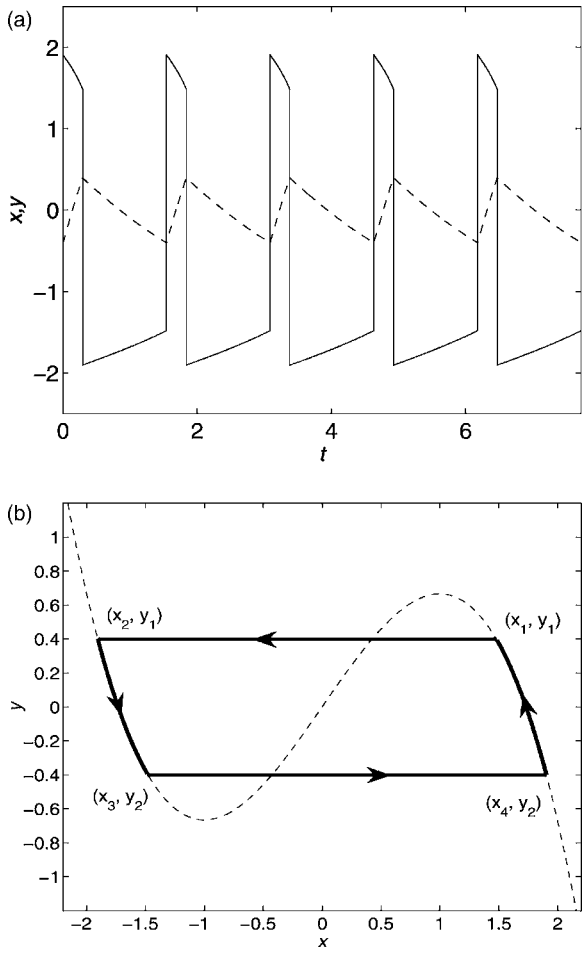

FIG. 9. Asymptotic limit cycle in SISR for $a=1.05$ and $\beta=0.1842$, corresponding to the parameters of the simulation in Figs. 2(b) and 2(d). In (a), the solid lines show $x(t)$ and the dashed lines show $y(t)$ obtained from the asymptotics. In (b), the thick solid lines with arrows indicate the limit cycle, and the dashed line is the x nullcline.

This can result in the emergence of a limit cycle which is radically different from the one in CR. The phase portrait of this limit cycle is composed of the two portions of the stable branches of the x nullcline between $y=y_1(\beta)$ and $y=y_2(\beta)$, together with the horizontal line joining these branches at y_1 and y_2; see Fig. 9. The period of the cycle is asymptotically the sum of the times it takes for the deterministic dynamics to go from y_1 to y_2 on S_L and from y_2 to y_1 on S_R, obtained from (6):

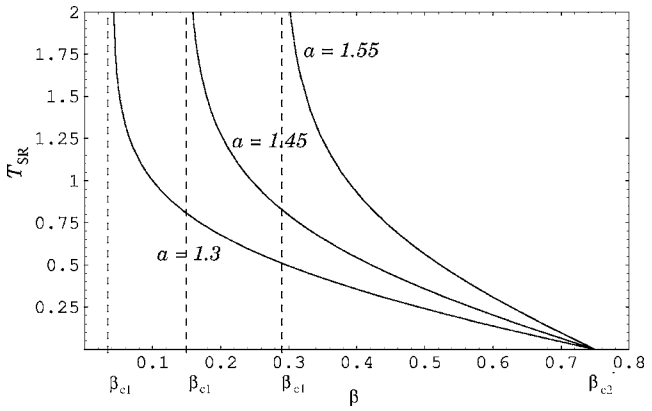

FIG. 10. Dependence of T on β (for a few values of a) for the SISR limit cycle obtained from the asymptotic theory.

$$T_{\mathrm{SR}}(\beta,a)=\int_{x_2(\beta)}^{x_3(\beta)}\frac{1-x^2}{x+a}dx+\int_{x_4(\beta)}^{x_1(\beta)}\frac{1-x^2}{x+a}dx, \qquad (26)$$

where $x_1=x_+(y_1), x_2=x_-(y_1), x_3=x_-(y_2)$, and $x_4=x_+(y_2)$. Once again, we can compute $T_{\mathrm{SR}}(\beta,a)$ parametrically in terms of x_1; see Fig. 10 for the dependence of T on β for a few values of a. Let us emphasize that the period of the obtained limit cycle depends non-trivially on the parameters β and a, and, therefore, can be controlled by the noise without significantly affecting the limit cycle coherence (see also [21]). The obtained limit cycle for $a=1.05$ and $\beta=0.1842$ shown in Fig. 9 corresponds to the parameters of the simulation in Figs. 2(b) and 2(d).

Note that the preceding arguments are valid only when $y_\star<y_2$, that is, when the point $y=y_2$ can be reached by the slow dynamics on S_L governed by (6). In view of the monotonicity of $\Delta V_-(y)$, this will happen when $\beta>\beta_{c1}(a)=\Delta V_-(y_\star)$. On the other hand, we must also have $y_2<y_1$, which is violated for $\beta\geqslant\beta_{c2}=\frac{3}{4}$ ($y_1=y_2=0$ at $\beta=\beta_{c2}$). If β is chosen larger than β_{c2}, then there is a region of y values for which the system can jump either left or right on the slow deterministic time scale, in which case we get nothing like a coherent orbit. Thus the deterministic limit cycle exists when $\beta\in(\beta_{c1},\beta_{c2})$. It is not difficult to see that this interval is not empty whenever $a<\sqrt{3}$, i.e., when $y_\star<0$.

Summarizing, the limit cycle due to SISR arises when

$$\varepsilon\ll 1,\quad \delta_1\ll 1,\quad 1<|a|<\sqrt{3}, \qquad (27)$$

provided that

$$\beta=\tfrac{1}{2}\delta_1^2\ln\varepsilon^{-1}=O(1),\quad \beta\in(\beta_{c1},\beta_{c2}). \qquad (28)$$

Compare this to the numerics in Fig. 2. It is predicted that the system jumps at $y_1=-y_2=0.4015$, which would give a period $T_{\mathrm{SR}}=1.534$ from the asymptotic theory above. In reasonable agreement with the theory, the system is jumping at $y_1=0.5\pm0.1$ and $y_2=-0.45\pm0.07$, but typically a little later than the prediction. Also, the observed average period of the cycle is about 25% more than the theoretical prediction. We attribute this to the fact that $\delta_1=0.2$ in the simulations, which is not very small in practice.

V. SELF-INDUCED STOCHASTIC RESONANCE NEAR HOPF BIFURCATION

Note that SISR is easier to realize when $b\to 0+$, since in this case

$$\beta_{c1}=\tfrac{4}{3}b^3+O(b^4), \qquad (29)$$

and so $\beta_{c1}\to 0$ as $b\to 0+$. So, smaller and smaller amounts of noise are sufficient to initiate SISR as one approaches the Hopf bifurcation. The SISR limit cycle then becomes closer and closer to the CR limit cycle, as we have to the leading order

$$y_1=\frac{2}{3}-\left(\frac{3\beta}{4}\right)^{2/3}, \qquad (30)$$

$$T_{\mathrm{SR}}=3-2b\ln\left[\left(\tfrac{3}{4}\beta\right)^{1/3}-b\right], \qquad (31)$$

when

$$\frac{b^3}{\ln\varepsilon^{-1}}\lesssim\delta_1^2\ll\frac{1}{\ln\varepsilon^{-1}}. \qquad (32)$$

Therefore, $T_{SR}\to 3$ for $b\to 0$ and β fixed, and the limit cycle becomes the same as one for CR. On the other hand, even in the limit of $a\to 1+$ and $\beta\to 0$ it is still possible to obtain a limit cycle from SISR that will be qualitatively different from the one in CR. For this, one needs to choose $b\to 0$ and $\beta\to 0$ jointly in a way that $\beta-\beta_c=O(e^{-cb^{-1}})$; see (29) and (31). Then the trajectory will "stick" in the neighborhood of the fixed point, but for a fixed deterministic $O(1)$ time, before jumping onto S_R.

VI. THE COMBINED SITUATION

Let us now consider the situation in which both δ_1 and δ_2 are nonzero, i.e, we add noise to both equations (1a) and (1b). First, it is clear that the CR mechanism will still require that $b=a-1\to 0+$, as well as $\delta_1\to 0, \delta_2\to 0$. Therefore, CR cannot occur if a is bounded away from 1. In contrast, SISR does not require that the system be near the bifurcation threshold, so it will still be feasible for those values of a to have a deterministic limit cycle, provided that δ_1 scales as in (21). Furthermore, it is clear that the coherence of the resulting limit cycle will not be affected by $\delta_2\neq 0$, as long as it also vanishes in the limit. Hence, the SISR takes over CR when a is not close to 1.

On the other hand, if $b=a-1\to 0+$, CR and SISR may compete. But since the graph of the limit cycle of SISR is always located inside the one of CR [compare Figs. 3 and 9(b)], provided only that the scalings in (27) (together with $\delta_2\ll 1$) are satisfied, SISR will again dominate CR. In fact, the only way for the limit cycle of CR to be observable is that the amplitude of the noise in (1a) be so small that the limit cycle in SISR becomes indistinguishable from the one in CR, as discussed in Sec. V.

VII. CONCLUSIONS

In conclusion, we have performed a careful examination of two different mechanism by which noise may induce new

coherent behavior in excitable systems, coherence resonance (CR) and the self-induced stochastic resonance (SISR). Using asymptotic techniques and numerical simulations, we have identified the distinguished limits in which the considered effects become *perfectly* coherent. We also showed that these two mechanisms have different origins and lead to qualitatively different behaviors.

The results of our analysis can be summarized as follows. Both CR and SISR rely on the strong separation of time scales between the excitatory and the recovery variables, $\varepsilon \ll 1$, and require a sufficient amount of noise for their operation. However, this is where the similarity between the two mechanisms ends.

To produce a quasideterministic limit cycle behavior, as we showed in Sec. III, CR relies on the closeness of the system to the Hopf bifurcation threshold. CR is robust in the sense that the coherence of the obtained limit cycle is rather insensitive to the time scale separation ratio between the fast and the slow variable (the value of $\varepsilon \ll 1$), and the amplitude of the noise (the value of $\delta_2 \ll 1$). On the other hand, in order for CR to be feasible, the system has to be tuned to be near the threshold of Hopf bifurcation ($a \to 1+$), and the distance away from the bifurcation threshold directly affects the degree of coherence of the cycle. Once the system is near the bifurcation point, any sufficiently large amount of noise (but not too large to overwhelm the entire dynamics) will be capable of inducing the limit cycle behavior. Thus, in CR the noise plays the role of essentially "smearing out" the region in the parameter space separating the deterministic limit cycle parameter region from that of excitability [31], making the system "feel" right before bifurcation the deterministic limit cycle emerging right after bifurcation (for $\varepsilon \to 0$).

In contrast, as we showed in Sec. IV, SISR is a stochastic resonance-type phenomenon that does not rely on the closeness to any bifurcation point. Thus SISR is robust in the sense that it does not require fine-tuning of the bifurcation parameters (in the considered example the value of a). The characteristics of the induced limit cycle however depend nontrivially both on the time scale separation ratio ε (weakly via its logarithm) but more importantly on the amplitude of the noise (the value of δ_1). This signifies a more subtle role of the noise in the generation of the coherent dynamics in the SISR mechanism. We also noted in Secs. V and VI that, topologically, SISR is more robust than CR because the graph of the SISR limit cycle is located inside the CR one. Thus CR can only be observed if the noise amplitude in (1a) is small enough.

Finally, let us point out an interesting feature of both CR and SISR limit cycles observed numerically. In the case of CR, the limit cycle appears to be very coherent in the phase plane; see Fig. 2(a). However, a look at the time series as well as the interspike time interval histogram shown in Fig. 1(c) shows a significant degree of incoherence in the timing of the successive cycles. On the other hand, in the case of SISR the phase portrait is visibly affected by the noise, more so than in CR, see Fig. 2(b); yet, the interspike time interval is very coherent, more so than in CR, see Fig. 1(d). The sharper coherence level for the SISR limit cycle compared to the CR limit cycle at the same noise level can also be seen from the histograms shown in Figs. 1(a)–1(d).

We note that both mechanisms of noise-induced coherence studied in this paper can have profound implications to the way biological systems operate in noisy environments or respond to highly irregular (noiselike) signals. This is especially true for the SISR mechanism, in which the amplitude of the noise plays the role of a control parameter and, therefore, its variations can lead to observably different coherent behaviors of the same dynamical system. Moreover, the SISR mechanism may in fact be used to detect the level of "irregularity" of a noiselike signal by converting that signal into a frequency-encoded periodic output. This is highly reminiscent of the way information is processed throughout the nervous system. The observed structural instability of excitable systems with respect to small noisy perturbations is also a warning to modelers. Quite dramatically, our results demonstrate that in the presence of noise the underlying dynamical model of a coherent oscillatory behavior does not have to possess a limit cycle, contrary to the currently accepted modeling dogma [7,35].

ACKNOWLEDGMENTS

E.V.-E. is partially supported by NSF via Grants DMS02-09959 and DMS02-39625, and by ONR via Grant N00014-04-1-0565. C.B.M. is partially supported by NSF via Grant DMS02-11864. W.E. is partially supported by ONR via Grant N00014-01-1-0674.

[1] M. I. Freidlin and A. D. Wentzell, *Random Perturbations of Dynamical Systems* (Springer-Verlag, New York, 1984).
[2] T. Wellens, V. Shatokhin, and A. Buchleitner, Rep. Prog. Phys. **67**, 45 (2004).
[3] J. M. G. Vilar, H. Y. Kueh, N. Barkai, and S. Leibler, Proc. Natl. Acad. Sci. U.S.A. **99**, 5988 (2002).
[4] T. Takahata, S. Tanabe, and K. Pakdaman, Biol. Cybern. **86**, 403 (2002).
[5] J. Paulsson, O. J. Berg, and M. Ehrenberg, Proc. Natl. Acad. Sci. U.S.A. **97**, 7148 (2000).
[6] J. S. Marchant and I. Parker, EMBO J. **20**, 65 (2001).
[7] J. Keener and J. Sneyd, *Mathematical Physiology* (Springer-Verlag, New York, 1998).
[8] *Chemical Waves and Patterns*, edited by R. Kapral and K. Showalter (Kluwer, Dordrecht, 1995).
[9] A. S. Mikhailov, *Foundations of Synergetics* (Springer-Verlag, Berlin, 1990).
[10] A. S. Pikovsky and J. Kurths, Phys. Rev. Lett. **78**, 775 (1997).
[11] A. Neiman, P. I. Saparin, and L. Stone, Phys. Rev. E **56**, 270 (1997).
[12] S.-G. Lee, A. Neiman, and S. Kim, Phys. Rev. E **57**, 3292 (1998).

[13] J. R. Pradines, G. V. Osipov, and J. J. Collins, Phys. Rev. E **60**, 6407 (1999).
[14] K. Miyakawa and H. Isikawa, Phys. Rev. E **66**, 046204 (2002).
[15] G. Giacomelli, M. Giudici, S. Balle, and J. R. Tredicce, Phys. Rev. Lett. **84**, 3298 (2000).
[16] J. B. Gao, W. W. Tung, and N. Rao, Phys. Rev. Lett. **89**, 254101 (2002).
[17] V. V. Osipov and E. V. Ponizovskaya, Phys. Lett. A **238**, 369 (1998).
[18] V. V. Osipov and E. V. Ponizovskaya, Phys. Rev. E **61**, 4603 (2000).
[19] T. Tateno and K. Pakdaman, Chaos **14**, 511 (2004).
[20] B. Lindner, J. Garcia-Ojalvo, A. Neiman, and L. Schimansky-Geier, Phys. Rep. **392**, 321 (2004).
[21] C. B. Muratov, E. Vanden Eijnden, and W. E, Physica D (to be published).
[22] M. I. Freidlin, J. Stat. Phys. **103**, 283 (2001).
[23] J. Grasman, *Asymptotic Methods for Relaxation Oscillations and Applications* (Springer, Berlin, 1987).
[24] E. F. Mishchenko and N. K. Rozov, *Differential Equations with Small Parameters and Relaxation Oscillations* (Plenum Press, London, 1980).
[25] J. Guckenheimer and P. Holmes, *Nonlinear Oscillations, Dynamic Systems, and Bifurcations of Vector Fields* (Springer-Verlag, New York, 1983).
[26] S. M. Baer and T. Erneux, SIAM J. Appl. Math. **46**, 721 (1986).
[27] S. M. Baer and T. Erneux, SIAM J. Appl. Math. **52**, 1651 (1992).
[28] B. S. Kerner and V. V. Osipov, *Autosolitons* (Kluwer, Dordrecht, 1994).
[29] *Oscillations and Traveling Waves in Chemical Systems*, edited by R. J. Field and M. Burger (Wiley Interscience, New York, 1985).
[30] Hu Gang, T. Ditzinger, C. Z. Ning, and H. Haken, Phys. Rev. Lett. **71**, 807 (1993).
[31] W.-J. Rappel and S. H. Strogatz, Phys. Rev. E **50**, 3249 (1994).
[32] K. Wiesenfeld, D. Pierson, E. Pantazelou, C. Dames, and F. Moss, Phys. Rev. Lett. **72**, 2125 (1994).
[33] J. J. Collins, C. C. Chow, and T. T. Imhoff, Nature (London) **376**, 236 (1995).
[34] L. Gammaitoni, P. Hänggi, P. Jung, and F. Marchesoni, Rev. Mod. Phys. **70**, 223 (1998).
[35] A. Goldbeter, Nature (London) **420**, 238 (2002).
[36] We use the standard forward Euler discretization of (1) with time step $\Delta t=0.01\varepsilon$ which is sufficient to resolve the fast dynamics of the system, with Box-Muller algorithm based on the lagged Fibonacci pseudorandom number generator to generate the noise. The quantity T is defined as the time interval between the successive crossings by the trajectory of the y axis in the lower half-plane of the phase space. Each histograms in Fig. 1 is obtained from 1000 cycles of the trajectory. The histograms are normalized to integrate to unity.
[37] It is not difficult to prove that all the trajectories starting at $\xi=0$ and $\eta<\eta_0$ for some $\eta_0<-1$ will reach $\xi=+\infty$ and $\eta=\eta_\infty$ at finite s.